JOURNAL OF GEOPHYSICAL RESEARCH, VOL. 113, D07211, doi:10.1029/2007JD009171, 2008

Saharan mineral dust transport into the Caribbean: Observed atmospheric controls and trends

O. M. Doherty,[1] N. Riemer,[1,2] and S. Hameed[1]

Received 14 July 2007; revised 31 October 2007; accepted 28 December 2007; published 15 April 2008.

[1] Each summer large amounts of mineral dust from the Sahara are transported across the Atlantic and arrive at the Caribbean with far-reaching implications for climate in this region. In this paper we analyze summer season interannual variability of North African mineral dust over the Caribbean using the Total Ozone Mapping Spectrometer (TOMS)/Nimbus 7 (1979–1992) and TOMS/Earth Probe (1998–2000) satellite aerosol data. We apply the ''centers of action'' approach to gain insight into the atmospheric controls on Saharan dust transport into the Caribbean and identify longitudinal displacement and pressure fluctuation of the Hawaiian High as well as longitudinal displacement of the Azores High as key players. In contrast, traditional indices such as the North Atlantic Oscillation and the Southern Oscillation are not correlated with the mineral dust variations over the Caribbean region. We utilize National Centers for Environmental Prediction/National Center for Atmospheric Research reanalysis to investigate the underlying physical mechanisms and to identify meteorological conditions that correspond to high and low dust loads. Our analysis shows that two different transport routes from distinct source regions are responsible for transporting mineral dust into the Caribbean: a northern mode in which dust mobilized from the Sahara travels westward controlled primarily by the Azores High and a southern mode in which intense dust clouds originating in the Sahel region travel over the Gulf of Guinea to reach the Caribbean. The latter is controlled primarily by teleconnections with the Hawaiian High.

Citation: Doherty, O. M., N. Riemer, and S. Hameed (2008), Saharan mineral dust transport into the Caribbean: Observed atmospheric controls and trends, *J. Geophys. Res.*, *113*, D07211, doi:10.1029/2007JD009171.

1. Introduction

[2] During summer large amounts of mineral dust are transported from sources in North Africa over the Atlantic to the Caribbean Sea. While first documented in 1846 [*Darwin*, 1846], atmospheric transport of Saharan mineral dust has occurred over geological timescales, having been found in long-term ice core samples [*Fischer*, 2001]. The long-range transport of mineral dust over the Atlantic is possible because of the existence of the so-called Saharan air layer, an elevated layer of Saharan air which extends over large portions of the North Atlantic between the Sahara and North America [*Prospero and Carlson*, 1972; *Carlson and Prospero*, 1972]. This layer of warm, dry air occurs from late spring until early fall above the marine boundary layer and can extend to about 5000 m thus allowing for prolonged residence time and advection of mineral dust over the greatest distance [*Petit et al.*, 2005].

[3] African mineral dust plays an important role in many biogeochemical systems [*Arimoto*, 2001]. It is thought to be responsible for the formation of the soils of many Caribbean islands and the Amazon Basin [*Herwitz et al.*, 1996], and it provides key nutrients for oceanic phytoplankton [*Jickells*, 1999]. It exerts a radiative forcing on the climate and has been linked with the frequency and intensity of Atlantic hurricanes [*Landsea and Gray*, 1992; *Dunion and Velden*, 2004; *Lau and Kim*, 2007]. Moreover, dust particles are likely to interact with the microphysics of clouds [*Rosenfeld et al.*, 2001; *Mahowald et al.*, 2003; *Levin et al.*, 2005].

[4] Ground observations at Barbados [*Prospero and Lamb*, 2003] suggest that the quantity of Saharan mineral dust in the atmosphere has been increasing, possibly in response to the continuous drought in the Sahel and new desert sources [*Mahowald et al.*, 2002]. The variability and trend of mineral dust transport from Africa over the Atlantic has far-reaching implications for the regional climate of the tropical Atlantic and the Caribbean [*Petit et al.*, 2005]. Because of its wide range of impacts on regional and intercontinental scales, it is important to understand the variability of dust transport over the Atlantic.

[5] It has been pointed out before that the variability of mineral dust in the Caribbean region is a result of many processes, including variations in dust emission in the source regions, changes in the transport paths, and changes in the amount of dust removed during transport by wet

[1] School of Marine and Atmospheric Science, Stony Brook University, Stony Brook, New York, USA.
[2] Now at Department of Atmospheric Sciences, University of Illinois at Urbana-Champaign, Urbana, Illinois, USA.

0148-0227/08/2007JD009171$09.00

deposition [*Prospero and Lamb*, 2003]. Previous attempts to explain the variability and trends in intercontinental transport of Saharan mineral dust have focused on the North Atlantic Oscillation (NAO) [*Chiapello et al.*, 2005; *Moulin et al.*, 1997] or El Niño–Southern Oscillation (ENSO) [*Prospero and Nees*, 1986]. The NAO has been shown to influence precipitation and wind patterns in regions of the Atlantic controlling dust transport [*Ginoux et al.*, 2004], especially in winter [*Chiapello and Moulin*, 2002]. ENSO affects precipitation over the Sahel [*Janicot et al.*, 1996; *Evan et al.*, 2006] and via a series of complex interacting processes affects emission and transport of dust from the source region [*Prospero and Nees*, 1986]. However, the NAO and ENSO do not explain the variability of mineral dust over the Caribbean region during summer, as we will show in section 3.3 of our analysis.

[6] While the NAO is a useful concept to explain the variability of dust during winter, it is less useful during summer, as the Icelandic Low ceases to be important [*Ginoux et al.*, 2004]. Since the summer season is the season of greatest dust transport to the Caribbean, it is important to establish conceptual mechanisms through which we can explain the variability in dust emission and transport. In order to address the summer variability, we take a new approach in this study and analyze satellite-derived dust observations by using the "centers of action" approach [*Piontkovski and Hameed*, 2002; *Hameed and Piontkovski*, 2004; *Riemer et al.*, 2006]. This approach will give us direct insight into the physical processes that govern the amount of mineral dust that arrives in the Caribbean.

[7] The centers of action (COA) are the large semipermanent pressure systems seen in the global distribution of sea level pressure [*Rossby*, 1939], such as the Azores High or the Icelandic Low, dominating the atmospheric circulation over a large region. Each COA is characterized by three indices: the longitudinal and latitudinal positions of its center of gravity and its central pressure. Hence, in contrast to the NAO, the COA approach makes use of the information on position as well as pressure. It therefore provides additional degrees of freedom so as to more directly explain the interannual variations of aerosol load in a specific region [*Riemer et al.*, 2006].

[8] We focus our investigation on a region bounded by 10°N–20°N and 70°W–59°W. The box was so chosen to include the island of Barbados where ground observations have been kept since the 1960s [*Prospero and Lamb*, 2003].

2. Methods and Data

2.1. Total Ozone Mapping Spectrometer Aerosol Index

[9] Previous studies have demonstrated that Total Ozone Mapping Spectrometer (TOMS) satellite data clearly show mineral dust, carbonaceous aerosol from biomass burning, and anthropogenic aerosol [*Torres et al.*, 2002; *Prospero et al.*, 2002; *Massie et al.*, 2004; *Washington and Todd*, 2005] over the continents and the subsequent aerosol transport over the ocean [*Herman et al.*, 1997; *Chiapello et al.*, 1999; *Chiapello and Moulin*, 2002]. The aerosol index (AI) from the TOMS instrumentation acts as a semiquantitative index of the vertically integrated atmospheric aerosol mass and is defined as

$$\mathrm{AI} = -100\{\log_{10}\left[(I_{317.5}/I_{331.2})_{\mathrm{meas}}\right] - \log_{10}\left[(I_{317.5}/I_{331.2})_{\mathrm{calc}}\right]\}, \quad (1)$$

where I_{meas} is the measured backscattered radiance at a given wavelength and I_{calc} is the radiance calculated at that wavelength assuming a purely gaseous atmosphere. Positive values of AI correspond to UV absorbing aerosols. In earlier versions of TOMS AI, negative values were generated representing nonabsorbing scattering aerosols but are no longer provided. A known shortcoming of the TOMS data is that the AI values are affected by the aerosol layer altitude [*Herman et al.*, 1997]. However, our study is limited to the summer season, where intraseasonal variability in the aerosol layer height is assumed to be less than the variability between seasons [*Cakmur et al.*, 2001; *Hsu et al.*, 1999]. It is also assumed that the height of the aerosol layer does not change significantly from year to year and that synoptic-scale variability is removed by examining seasonal means. Furthermore, it is known that small values of AI could be due to cloud contamination [*Torres et al.*, 1998, 2002]. We will address this problem in section 3.1 by introducing certain thresholds that exclude small AI values which potentially could represent clouds and not small amounts of aerosol.

[10] For this study the most recent version (version 8) of the TOMS AI daily data from both the Nimbus 7 (1979–1993) and Earth Probe (1997–2004) satellites is used. Owing to sensor calibration issues on Earth Probe [*Kiss et al.*, 2007], values after summer 2000 are excluded. We also exclude the season of 1997 since the missing data in our region of interest reach about 50% occurrence. Hence our analysis includes the years 1979–1993 and 1998–2000.

2.2. Centers of Action Approach

[11] The large-scale semipermanent pressure centers known as "centers of action" were introduced by *Rossby* [1939]. Each COA exhibits a characteristic seasonal cycle. During winter the Icelandic Low, the Aleutian Low, the Azores High, and the Siberian High are most pronounced. In summer the low-pressure centers weaken, and the Hawaiian High and the Azores High dominate. Additionally, in the summer, the South Asia Low, related to the Indian monsoon, forms as a center of low pressure. In addition to a weakening and strengthening of the pressure centers, there is also displacement; for example, in summer the Hawaiian High and the Azores High move to the east compared to the winter season. The position and the strength of the COA are captured by three indices representing its longitude, latitude, and pressure.

[12] Recently, this approach has successfully been used to explain the role of the movement and intensity of individual atmospheric COAs on such varied biogeochemical systems as copepod abundance [*Piontkovski and Hameed*, 2002], the variation in the location of the Gulf Stream [*Hameed and Piontkovski*, 2004], and the variability of the transport of African dust [*Riemer et al.*, 2006]. Compared to the traditional NAO approach [*Hurrell*, 1995], the COA are decoupled, and their meridional and zonal movement are considered independently as are the variations in the intensity of the pressure. The approach is well described by

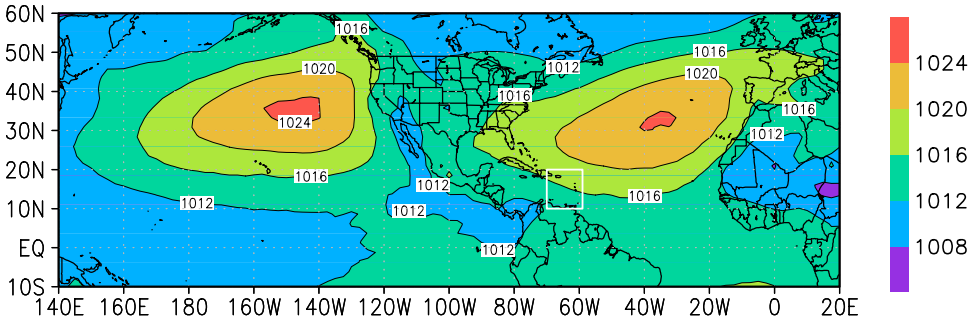

Figure 1. Average surface level pressure distribution for June, July, and August of 1975–2005. Source is National Centers for Climate Prediction (NCEP) reanalysis [*Kalnay et al.*, 1996].

Piontkovski and Hameed, Hameed and Piontkovski, and Riemer et al., as well as by *Hameed et al.* [1995], but it is briefly summarized as follows.

[13] The pressure index I_p is defined as an area-weighted pressure departure from a threshold value over the domain (I, J):

$$I_p = \frac{\sum_{i,j=1}^{I,J} (P_{i,j} - P_t) \cos\phi_{i,j} (-1)^M \delta_{i,j}}{\sum_{i,j=1}^{I,J} \cos\phi_{i,j} \delta_{i,j}}, \quad (2)$$

where $P_{i,j}$ is the sea level pressure value at a grid point (i,j), P_t is the threshold sea level pressure value (P_t = 1014 hPa), and $\varphi_{i,j}$ is the latitude of grid point (i,j). $M = 0$ for the Azores High and 1 for the Icelandic Low; $\delta = 1$ if $(-1)^M(P_{i,j} - P_t) > 0$, and $\delta = 0$ if $(-1)^M(P_{i,j} - P_t) < 0$. The latitudinal index I_φ is defined as

$$I_\phi = \frac{\sum_{i,j=1}^{I,J} (P_{i,j} - P_t)\phi_{i,j} \cos\phi_{i,j} (-1)^M \delta_{i,j}}{\sum_{i,j=1}^{I,J} (P_{i,j} - P_t) \cos\phi_{i,j} (-1)^M \delta_{i,j}}. \quad (3)$$

The longitudinal index I_λ is defined analogously. The location indices thus give pressure-weighted mean latitudinal and longitudinal positions of the centers. For the surface pressure data we use gridded National Centers for Environmental Prediction (NCEP) reanalysis data [*Kalnay et al.*, 1996].

[14] Figure 1 shows the distribution of June, July, and August (JJA) surface pressure averaged over 1975–2000 for the region around the Caribbean. We see the dominating presence of two COAs: the Azores High to the east, characterized by sea level pressure >1020 hPa in its center over the north Atlantic, and the Hawaiian High to the west. Both the Hawaiian High and the Azores High migrate from season to season and year to year and vary with the strength of the Northern Hemisphere Hadley circulation [*Lydolph*, 1985]. Obviously, the strength and position of the Azores High directly influences circulation and precipitation in the Atlantic Basin, the Caribbean, and the Sahara [*Rossby*, 1939; *Angell and Korshover*, 1974]. The influence of the Hawaiian High on the Atlantic is illustrated by the teleconnections in the Northern Hemisphere midlatitude summer circulation investigated by *Ding and Wang* [2005] and *Zhao et al.* [2007] and is discussed further in section 3.3.

3. Results

3.1. Trends of Aerosol Load Over the Caribbean

[15] Previous work has suggested that the westward transport of Saharan mineral dust depends strongly on the season [*Chiapello et al.*, 2005; *Husar et al.*, 1997; *Prospero*, 1999]. We confirm this by averaging the TOMS daily data for the individual months over our area of interest. Figure 2 shows the climatology of the TOMS AI for the years 1979–

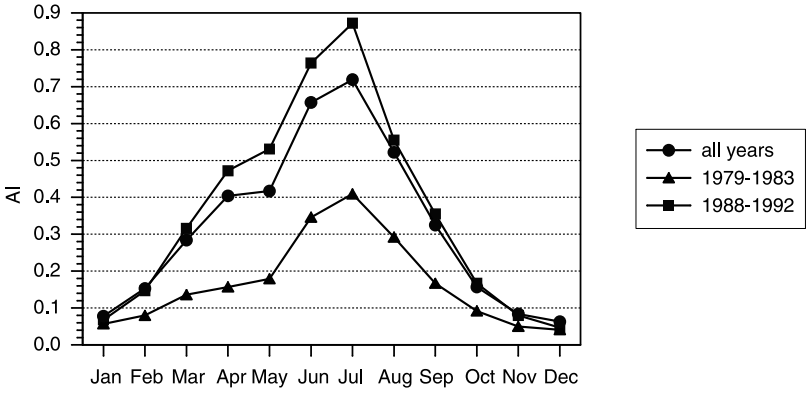

Figure 2. Monthly mean AI values spatially averaged over the region 59°–70°W, 10°–20°N and temporally averaged over different time periods. "All years" refers to the time periods 1979–1993 and 1998–2000.

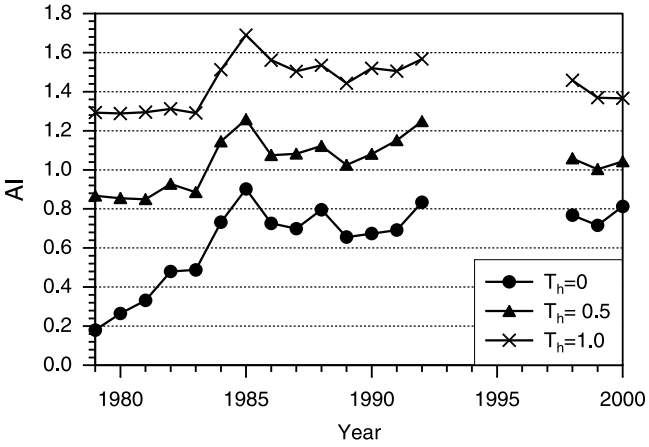

Figure 3. June–July–August averages of AI over the region 59°–70°W, 10°–20°N for different thresholds T_h applied to the daily AI values before averaging.

1993 and 1998–2000 (circles). A clear seasonal cycle is observed with maximum dust levels occurring during the summer months of June, July, and August and minimum dust levels observed in the winter months of December, January, and February. This cycle matches closely with ground-based observations taken in Barbados by *Prospero and Nees* [1986], who observed a similar summer seasonal maximum and winter minimum.

[16] Figure 3 shows the seasonal averaged values for JJA of TOMS AI for 1979–1993 and 1998–2000 and for different thresholds (T_h = 0, 0.5, and 1). A threshold of T_h means that only daily values equal or larger than T_h are included in the temporal and spatial average. Applying thresholds has two purposes. First, it allows us to separate the strong dust events from the overall data. Second, since low AI values could be due to cloud contamination, by applying a threshold, we exclude potentially cloud-contaminated data [*Torres et al.*, 1998, 2002]. By applying T_h = 0.5 and T_h = 1, we exclude on average about 50% and 75% of data, respectively.

[17] Regardless of the threshold applied, we see an increase in AI from 1979 to 1985, this increase being more pronounced for lower T_h. From 1985 throughout the rest of the Nimbus 7 period the elevated level is maintained. The Earth Probe data suggest that a slight decrease has occurred in the later years of the record; however, its significance is not clear because we have only three data points.

[18] *Prospero and Lamb* [2003] find a similarly increasing trend in the Barbados data for the 1970s into the 1980s and relate this to the severe drought in the Sahel region since they find that the dust load in Barbados is anticorrelated with the Sahel precipitation index of the previous year. We will relate our results to these findings in section 3.3.

[19] Analysis of the trends during spring and fall show that not only the AI for JJA has increased but also the values for the months before and after the peak season have increased. The width of the peak in Figure 2 has clearly broadened between 1979–1983 and 1988–1992, strongly suggesting that the season of maximum dust in the Caribbean has lengthened. AI has increased not only during summer but throughout the whole year, with the largest increase in spring (factor of 3 for March, April, and May). Conditions formerly associated with summer-like AI were seen in March through September in the latter period. Quantitatively, a monthly mean of 0.3 was exceeded for only June, July, and August for 1979–1983, while this value is exceeded from March through September for 1988–1992. We conclude that the dusty summer season in the early 1980s was extended in duration to include spring and fall by the late 1980s. We do not include any of the Earth Probe record in this analysis for the following reasons. *Kiss et al.* [2007] find a small bias (~0.2) in the Earth Probe record relative to Nimbus 7, even during the early portion of the Earth Probe record (1996–2000). This bias is of critical importance for seasons in which the AI is low (i.e., winter and spring). Additionally, *Kiss et al.* [2007] find that the Earth Probe satellite undergoes a steady degradation into the 21st century. Therefore the Earth Probe record is not suitable for this trend analysis, and we limit our discussion to the Nimbus period.

[20] Several factors could be responsible for the lengthening of the dust season, e.g., increased emissions in the source regions and/or changes in the transport patterns. Treating North Africa as a source, we calculate the average AI for the region 5°N–30°N and 15°W–30°E for the individual months of the year (T_h = 0). The AI in the months April and May and September and October, i.e., immediately before and after the peak dust season in the Caribbean, indeed show an increase in the first part of the 1980s (Figure 4). This suggests that the observed lengthening of the dust season in the Caribbean is at least partially due to increased emissions in the source region. TOMS lacks the ability to distinguish between biomass-burning aerosols and mineral dust aerosols; thus it is possible that some of the increase in aerosols observed in the Caribbean are not mineral dust but are rather biomass-burning particles.

[21] In addition, a shift in the transport path over the Atlantic could have taken place. To explore this hypothesis, we show the composite difference of the meridional wind field at 700 hPa, where we subtract the 5-year average for March, April, and May 1979–1983 from the 5-year average for March, April, and May 1989–1993 (Figure 5). The

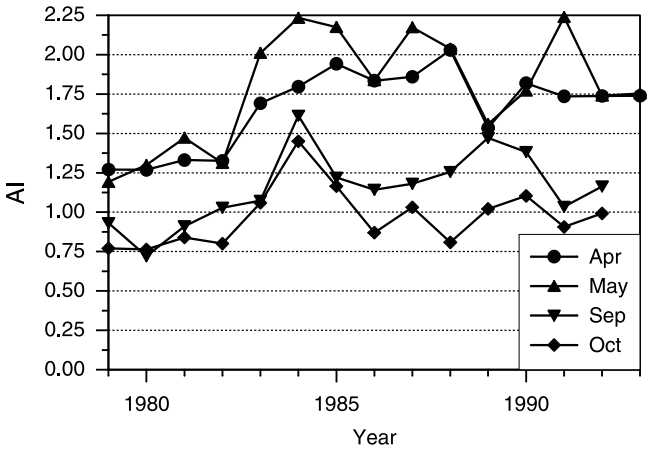

Figure 4. Monthly AI averages for the North African source region 5°N–30°N and 15°W–30°E (T_h = 0).

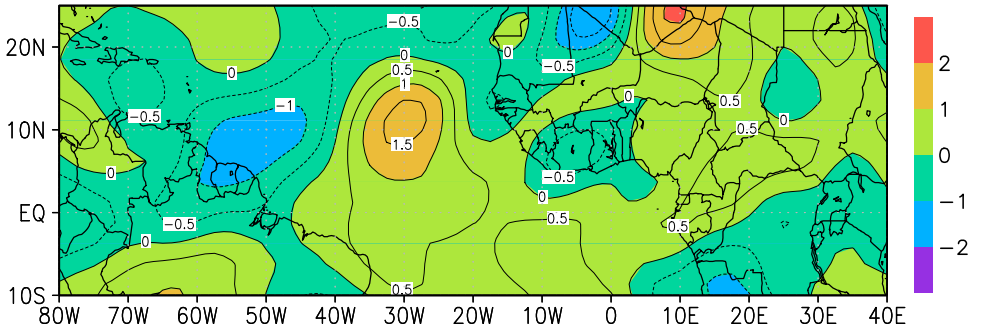

Figure 5. Differences of meridional velocity for March, April, and May. Average of 1989–1993 minus 1979–1983. Source is NCEP reanalysis [*Kalnay et al.*, 1996].

results show a cyclonic anomaly in the mid-Atlantic which has a southerly component from the equator to 15°N between 40°W and 0°W. This means that the dust plume in spring (which extends more to the south compared to summer [*Husar et al.*, 1997]) has shifted northward in the later time period, reaching the Caribbean earlier in the year. In summary, we conclude that both emissions and changes in transport have contributed to the prolonged dust season in the Caribbean; however, satellite limitations prevent us from ruling out appreciable contributions from biomass burning.

3.2. Correlations With COAs

[22] To gain insight into the atmospheric control of the dust load over the Caribbean, we apply the COA approach to the TOMS AI record in our Caribbean box. Table 1 shows the same-year correlation coefficients between the seasonally averaged AI and indices of Hawaiian High and Azores High, with statistically significant results denoted. Additionally, we consider different values of daily AI thresholds T_h. Three variables are significantly correlated: the Azores High longitude (at 90%), the Hawaiian High longitude (at 90%), and the Hawaiian High central pressure (at 95%). Dust levels in the Caribbean are seen to increase with a westward displacement of the Azores High, with a weakening of the Hawaiian High, and with an eastward displacement of the Hawaiian High. Moreover, the correlation coefficient depends on the AI threshold. For simplicity, Table 1 only displays the two extremes ($T_h = 0$ and $T_h = 1$), but this behavior is consistent for other thresholds in between. We realize that these correlations do not necessarily imply causation; in section 3.3 we attempt to shed light on the possible underlying physical mechanisms.

3.3. Atmospheric Controls

[23] In this section we discuss and examine the underlying physical processes for the case for $T_h = 0$ (i.e., including all data) and the case for $T_h = 1$ (i.e., only intense dust events) separately. We present composite figures with respect to horizontal wind field and precipitation showing the differences between the extremes of the positions and intensity of the relevant COA. We analyze the wind fields at 700 hPa since the aerosol transport off the coast of Africa during summer occurs approximately at this level [*Carlson and Prospero*, 1972; *Cakmur et al.*, 2001]. To produce these composite differences, we rank each COA index of the months June, July, and August to determine when the COA index was highest and lowest. The 10 months with the lowest COA indices and the 10 months with the highest COA indices are then defined as the "low months" and "high months," respectively (the lowest and highest 10 months correspond to approximately the twentieth and eightieth percentile, respectively). We then average the horizontal wind fields and precipitation for the low months and the high months and calculate the differences representing maximum dust in the Caribbean region. For the wind field data we use the NCEP reanalysis [*Kalnay et al.*, 1996]. For precipitation we use data from the Global Precipitation Climatology Project [*Alder et al.*, 2003].

3.3.1. Intense Dust Events Only ($T_h = 1$)

[24] If we focus on the intense dust events, the governing COA appears to be the Hawaiian High. Figures 6 and 7 show the composite differences of wind field at 700 hPa and precipitation for the extreme conditions of the Hawaiian High pressure and the Hawaiian High longitude, respectively.

[25] The pressure index of the Hawaiian High is negatively correlated with the AI for nearly every threshold level and is most strongly correlated for the highest values of T_h. A decrease in the strength of the Hawaiian High is associated with an increase in the quantity of mineral dust in the Caribbean. As seen in Figure 6, in the case in which we expect dust transport into the Caribbean to be maximized, there is enhanced westward flow over the Atlantic south of

Table 1. Correlation Coefficients of the AI With the Azores High and Hawaiian High Indices and the SOI and NAO Indices for the Periods 1979–1992 and 1998–2000[a]

T_h	AZ Lon	AZ Lat	AZ P	HA Lon	HA Lat	HA P	NAO	SOI
0	−0.42[b]	−0.11	−0.39	0.19	−0.06	−0.27	−0.19	−0.02
1.0	−0.37	−0.27	−0.19	0.43[b]	0.11	−0.49[c]	−0.09	0.001

[a]Summer averages include the months June to August. The AI is averaged over the area 10°–20°N, 59°–70°W. Abbreviations are Lon, longitude; Lat, latitude; P, pressure; NAO, North Atlantic Oscillation; and SOI, Southern Oscillation Index.
[b]Significant correlation at 90%.
[c]Significant correlation at 95%.

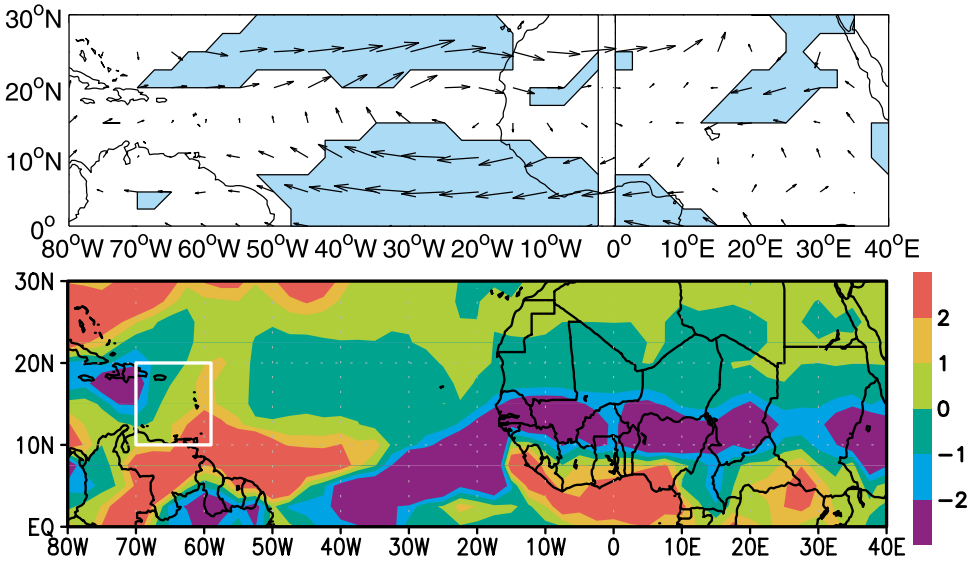

Figure 6. Composite difference in (top) 700 hPa winds and (bottom) precipitation for the 10 lowest Hawaiian High pressure index months minus the 10 highest Hawaiian High pressure months. The 10 highest and 10 lowest months correspond to the eightieth and twentieth percentile months. Conditions as shown represent conditions that will lead to increased dust in the Caribbean. Source is NCEP reanalysis [*Kalnay et al.*, 1996]. The shading represents significant differences in the wind fields.

10°N and a slight southward component off the coast of Africa toward the Atlantic. It appears that the pressure distribution associated with the Hawaiian High acts to reduce transport off the subtropical coast of Africa, while enhancing transport through the Gulf of Guinea. The corresponding precipitation composite difference shows that the intertropical convergence zone is displaced southward. This leads to drier conditions in the Sahel region favoring dust emissions.

[26] The longitude index of the Hawaiian High is positively correlated with the AI. Increasing values of the Hawaiian High longitude index imply an eastward displacement of this COA. Thus the positive correlation means that eastward movement of the Hawaiian High results in in-

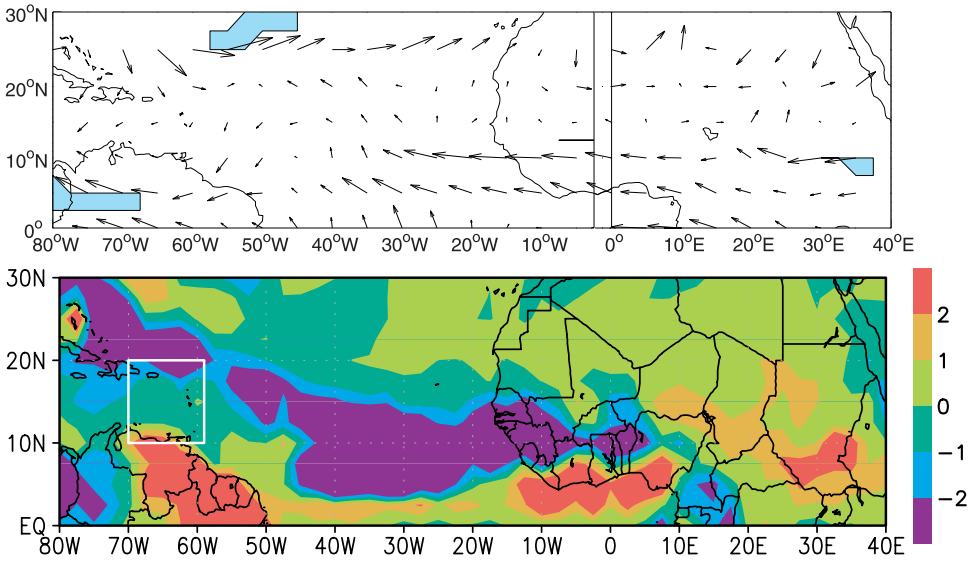

Figure 7. Composite difference in (top) 700 hPa winds and (bottom) precipitation for the 10 highest Hawaiian High longitude index months minus the 10 lowest Hawaiian High longitude months. The 10 highest and 10 lowest months correspond to the eightieth and twentieth percentile months. Conditions as shown represent conditions that will lead to increased dust in the Caribbean. Source is NCEP reanalysis [*Kalnay et al.*, 1996].

creased dust levels in the Caribbean. In the composite differences for the wind field at 700 hPa in Figure 7, we see an increased easterly wind component of up to 3 m s^{-1} between the equator and 10°N, which enhances the dust transport from the Sahel, similar to but more modestly than for the Hawaiian High central pressure composites. These wind anomalies, however, turn out not to be statistically significant. The corresponding precipitation composite shows a wide swath of decreased precipitation across the Caribbean, into the tropical North Atlantic, and into the Sahel. We relate this decreased precipitation to an increased subsidence over this area, which is prevalent when the Hawaiian High moves eastward (figure not shown). The Hawaiian High longitude appears to play an important role in determining the quantity of precipitation over the Caribbean and over the Atlantic, thus impacting the removal of dust by wet deposition. Overall, we conclude that the intense dust events are controlled by the Hawaiian High, both by its influence on precipitation and by its influence on the transport of dust from the Sahel via the southern transport path over the Gulf of Guinea.

[27] A question arises whether it is reasonable to expect that fluctuations in the Hawaiian High pressure system can influence winds over North Africa and the North Atlantic. Correlations at a distance are usually called teleconnections, especially those between tropical and extratropical atmospheric circulations [*Wallace and Gutzler*, 1981; *Mo and Livezey*, 1986; *Barnston and Livezey*, 1987; *Trenberth et al.*, 1998]. Most of the studies on teleconnections are for the boreal winter. Theoretical and modeling studies have shown that anomalies in ENSO sea surface temperatures influence midlatitude winter atmospheric anomalies by the propagation of Rossby waves. However, ENSO's teleconnection to Sahel rainfall variations has been detected for the summer season also [e.g., *Palmer*, 1986; *Bhatt*, 1989; *Janicot et al.*, 1996; *Rowell*, 2001]. *Gray and Landsea* [1994] showed that the Southern Oscillation index (SOI) is correlated with tropical cyclone activity in the Atlantic. This is evidence that the pressure fluctuations in the summer in the tropical Pacific influence winds and atmospheric pressure distributions in tropical western Africa. Variations in the Hawaiian High pressure system control the strength and the position of the trade winds and are highly correlated with fluctuations in the SOI. A circumglobal teleconnection pattern in the summer (June–September) circulation in the midlatitudes of the Northern Hemisphere was shown by *Ding and Wang* [2005], who analyzed (1948–2003) NCEP reanalysis data at 200 hPa. This teleconnection pattern has a zonal wave 5 structure and is seen to be in a waveguide associated with the westerly jet stream. The teleconnection pattern shows significant anomalies over the central Pacific (where the Hawaiian High system is located), the midlatitude Atlantic, North Africa, and several other regions around the globe. *Ding and Wang* [2005] found that the circumglobal teleconnection pattern has significant correlations with the Indian summer monsoon, and previously, *Shi* [1999] had reported a significant relationship between the Indian summer monsoon and the Hawaiian High pressure. The mechanism that maintains the circumglobal teleconnection pattern remains to be worked out; however, it shows that anomalies in the midlatitude Pacific are related to anomalies over the Atlantic and North Africa. In a recent investigation *Zhao et al.* [2007] defined the Asian-Pacific Oscillation, which is also a zonal teleconnection pattern over the extratropical Asian-Pacific region, using empirical orthogonal functions of summer mean tropospheric eddy temperature from the monthly European Centre for Medium-Range Weather Forecasts reanalysis. *Zhao et al.* [2007] noted that with higher Asian-Pacific Oscillation index the Hawaiian High pressure is stronger. The first empirical orthogonal function (EOF) mode exhibits an out-of-phase relationship between Asia and the North Pacific and has significant amplitudes over the midlatitudes of North America and the North Atlantic, while the second EOF mode has significant amplitudes over the tropical North Atlantic and North Africa. The relationships between the Hawaiian High with dust outflow from the Sahel reported in this paper are consistent with the relationships between North Atlantic and North African climate and pressure fluctuations in the Pacific reported by *Zhao et al.* [2007] and *Ding and Wang* [2005]. However, these teleconnections need to be investigated in general circulation models to clarify their underlying mechanisms.

3.3.2. All Data ($T_h = 0$)

[28] If we take all data into account (i.e., apply low thresholds), the longitude of the Azores High is significantly negatively correlated with AI over the Caribbean. A westward movement of the Azores High corresponds to increasing AI in the Caribbean. Figure 8 shows the composite differences of the 700 hPa wind field and precipitation. Increased easterlies, coming from the Saharan region north of about 15°N, are seen across much of the tropical North Atlantic. At the same time, the corresponding precipitation patterns show wetter conditions throughout the Sahel. This is expected since the subsidence over the Sahel is enhanced when the Azores High moves closer to Africa and vice versa. For this case, dust in the Caribbean is maximized despite higher precipitation in the Sahel. This can be reconciled by the fact that the dust for these conditions originates from the Sahara region, north of the Sahel. The conditions that are favorable for dust are created by the wind field not by precipitation, and the export from the Saharan desert plays the dominant role.

[29] In Table 1 we show the correlation coefficients between the seasonally averaged AI and the SOI and NAO index from the NOAA Climate Prediction Center. Clearly, the interannual variability of mineral dust in the Caribbean can be explained to a larger extent by the individual indices of the Hawaiian High and Azores High and is not greatly dependent on the same-year El Niño conditions nor the NAO system as a whole. Our composite analysis shows that the same-year correlations with the Hawaiian High and the Azores High are consistent with the wind and the precipitation patterns during transport.

[30] A previous study by *Prospero and Lamb* [2003] shows that previous-year precipitation in the Sahel region is anticorrelated with the dust load at Barbados. Since Sahel precipitation, in turn, has been shown to be influenced by ENSO [*Janicot et al.*, 1996; *Evan et al.*, 2006], there is an ENSO influence on dust in the Caribbean via this mechanism. When correlating the AI with Sahel precipitation of the previous year, we obtain correlation coefficients of

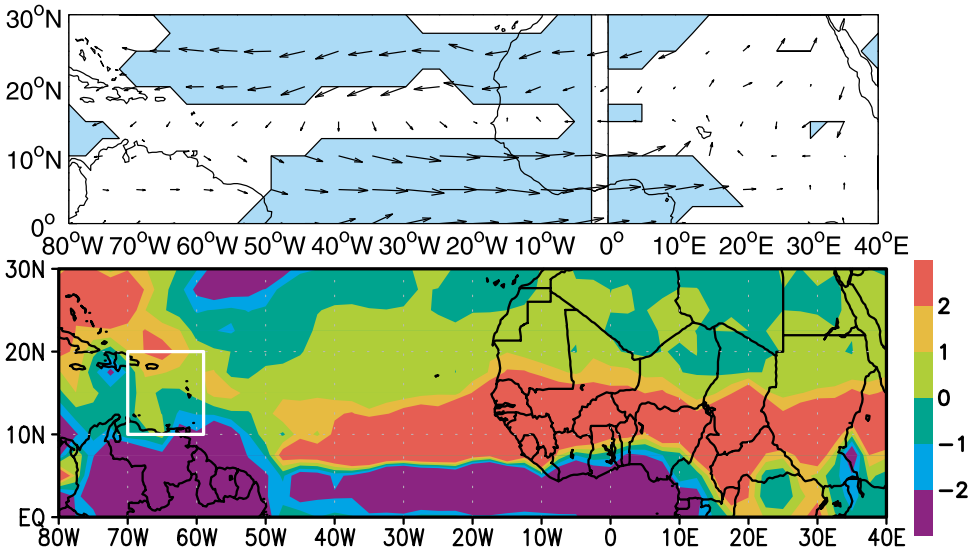

Figure 8. Same as Figure 6 but for Azores High longitude.

r = (−0.33, −0.46, and −0.48) for the AI thresholds T_h = (0, 0.5, and 1). For Sahel precipitation data we use the monthly mean rain gauge data set by *Hulme* [1994] and *Hulme et al.* [1998]. While there is no significant correlation of precipitation and AI when we include all data, we obtain a statistically significant result for intense dust events. This indicates that the occurrence of intense dust events is related to low precipitation in the Sahel in the previous year, whereas this relationship does not manifest itself when we include all the data. While these correlations are not necessarily the result of causation, they are consistent with our findings from above as intense dust events (T_h = 1) are related to dust export from the Sahel, whereas dust events with T_h = 0 originate from the Sahara.

[31] A possible explanation may be that a certain amount of dust is always exported from the Saharan desert and reaches the Caribbean regardless of the precipitation in the Sahel. On the other hand, for intense dust events to occur, low precipitation in the Sahel in the preceding year is required. Our results support a similar hypothesis put forward by *Chiapello et al.* [2005]. They conclude that the Sahel region is likely to be the controlling factor for the year-to-year variability of dust export. However, overall it should be noted that even the significant correlation for the intense dust events only explains about 23% of the variability. This is in contrast to *Prospero and Lamb* [2003], who report that about 56% of the variability of the Barbados May-to-September mean dust load can be explained by the prior-year precipitation in the Sahel, measured by the Sahel precipitation index.

4. Conclusions

[32] We have shown through use of long-term TOMS satellite data that both the quantity of dust and the length of the "dust season" in the Caribbean have increased during the 1980s and have plateaued into the 1990s. Since Earth Probe data degrade after 2000, no conclusion for the present state can be drawn. The prolonged season has two causes which occur simultaneously. First, the emissions have increased throughout the year, especially during spring; second, there has been a shift in transport patterns, so that the dust plume moves northward from its winter position earlier in the year.

[33] With the COA approach we identify a relationship between the Azores High and Hawaiian High and dust levels in the Caribbean during summer. Specifically, we were able to identify two different regimes of dust transport depending on the AI threshold applied to the daily data. When applying a zero (or low) threshold (i.e., by including all data), we find that the AI in the Caribbean is related to the east-west movement of the Azores High longitude. A composite analysis suggests that the westward movement of the Azores High greatly impacts the circulation of the tropical North Atlantic, enhancing easterly flow across the western Sahara and increasing dust transportation.

[34] The Hawaiian High, on the other hand, appears to play a significant role for intense dust events by impacting the distribution of precipitation from the Sahel to the Caribbean Basin. The Hawaiian High also influences the dust export by enhancing the flow over the Gulf of Guinea. In agreement with *Chiapello et al.* [2005] we conclude that for intense dust events in the Caribbean the Sahel region is an important factor.

[35] **Acknowledgments.** We thank Joe Propsero and his research group for sharing with us the Barbados mineral dust data set, and we are grateful to the anonymous reviewers for their thorough review of our manuscript.

References

Alder, R., G. Huffman, and A. Chang (2003), The Version-2 Global Precipitation Climatology Project (GPCP) monthly precipitation analysis (1979–present), *J. Hydrometeorol.*, *4*, 1147–1167.

Angell, J., and T. Korshover (1974), Quasi-biennial and long-term fluctuations in the centers of action, *Mon. Weather Rev.*, *102*, 669–678.

Arimoto, R. (2001), Eolian dust and climate: Relationships to sources, tropospheric chemistry, transport, and deposition, *Earth Sci. Rev.*, *54*, 29–42.

Barnston, A., and R. Livezey (1987), Classification, seasonality and persistence of low-frequency atmospheric circulation patterns, *Mon. Weather Rev.*, *115*, 1083–1126.

Bhatt, U. (1989), Circulation regimes of rainfall anomalies in the African–South Asian monsoon belt, *J. Clim.*, *2*, 1133–1144.

Cakmur, R., R. Miller, and I. Tegen (2001), A comparison of seasonal and interannual variability of soil dust aerosols over the Atlantic Ocean as inferred by the TOMS AI and AVHRR AOT retrievals, *J. Geophys. Res.*, *106*, 18287–18303.

Carlson, T., and J. Prospero (1972), The large-scale movement of Saharan air outbreaks over the northern equatorial Atlantic, *J. Appl. Meteorol.*, *11*, 283–297.

Chiapello, I., and C. Moulin (2002), TOMS and Meteosat satellite records of the variability of Saharan dust transport over the Atlantic during the last two decades (1979–1997), *Geophys. Res. Lett.*, *29*(8), 1176, doi:10.1029/2001GL013767.

Chiapello, I., J. Prospero, J. Herman, and N. Hsu (1999), Detection of mineral dust over the North Atlantic Ocean and Africa with the Nimbus 7 TOMS, *J. Geophys. Res.*, *104*, 9277–9291.

Chiapello, I., C. Moulin, and J. M. Prospero (2005), Understanding the long-term variability of African dust transport across the Atlantic as recorded in both Barbados surface concentrations and large-scale Total Ozone Mapping Spectromenter (TOMS) optical thickness, *J. Geophys. Res.*, *110*, D18S10, doi:10.1029/2004JD005132.

Darwin, C. (1846), An account of this fine dust which often falls on vessels in the Atlantic Ocean, *Q. J. Geol. Soc. London*, *2*, 26–30.

Ding, Q., and B. Wang (2005), Circumglobal teleconnection in the Northern Hemisphere summer, *J. Clim.*, *18*, 3483–3505.

Dunion, J., and C. Velden (2004), The impact of the Saharan air layer on Atlantic tropical cyclone activity, *Bull. Am. Meteorol. Soc.*, *85*, 353–365.

Evan, A., J. Dunion, J. Foley, A. Heidinger, and C. Velden (2006), New evidence for a relationship between Atlantic tropical cyclone activity and African dust outbreaks, *Geophys. Res. Lett.*, *33*, L19813, doi:10.1029/2006GL026408.

Fischer, H. (2001), Imprint of large-scale atmospheric transport patterns on sea-salt records in northern Greenland ice cores, *J. Geophys. Res.*, *106*, 23,977–23,984.

Ginoux, P., J. Prospero, O. Torres, and M. Chin (2004), Long-term simulation of global dust distribution with the GOCART model: Correlation with North Atlantic Oscillation, *Environ. Modell. Software*, *19*, 113–128.

Gray, W., and C. Landsea (1994), Predicting Atlantic Basin seasonal tropical cyclone activity by June 1, *Weather Forecasting*, *9*, 102–115.

Hameed, S., and S. Piontkovski (2004), The dominant influence of the Icelandic Low on the position of the Gulf Stream northwall, *Geophys. Res. Lett.*, *31*, L09303, doi:10.1029/2004GL019561.

Hameed, S., W. Shi, J. Boyle, and B. Santer (1995), Investigation of the centers of action in the North Atlantic and North Pacific in the ECHAM AMIP simulation, paper presented at the First International AMIP Scientific Conference, World Clim. Res. Programme, Monterey, Calif., 15–19 May.

Herman, J., P. Bhartia, O. Torres, B. Holben, D. Tanre, T. Eck, A. Smirnov, B. Chatenet, and F. Lavenu (1997), Global distribution of UV-absorbing aerosols from Nimbus 7/TOMS data, *J. Geophys. Res.*, *102*(D14), 16,911–16,922.

Herwitz, S., D. Muhs, J. Prospero, S. Mahan, and B. Vaughn (1996), Origin of Bermuda's clay-rich Quaternary paleosols and their paleoclimatic significance, *J. Geophys. Res.*, *101*, 23,389–23,400.

Hsu, N., J. Herman, O. Torres, B. Holben, D. Tanre, T. Eck, A. Smirnov, B. Chatelet, and F. Lavenu (1999), Comparison of the TOMS aerosol index with Sun-photometer aerosol optical thickness: Results and applications, *J. Geophys. Res.*, *104*, 6269–6279.

Hulme, M. (1994), Validation of large-scale precipitation fields in general circulation models, in *Global Precipitations and Climate Change*, edited by M. Desbois and F. Desalmand, pp. 387–406, Springer, Berlin.

Hulme, M., T. Osborne, and T. Johns (1998), Precipitation sensitivity to global warming: Comparison of observations with HadCM2 simulations, *Geophys. Res. Lett.*, *25*, 3379–3382.

Hurrell, J. (1995), Decadal trend in the North Atlantic Oscillation: Regional temperatures and precipitation, *Science*, *269*, 676–679.

Husar, R., J. M. Prospero, and L. Stowe (1997), Characterization of tropospheric aerosols over the oceans with the NOAA advanced very high resolution radiometer optical thickness operational product, *J. Geophys. Res.*, *102*, 16,889–16,909.

Janicot, S., V. Moron, and B. Fontaine (1996), Sahel droughts and ENSO dynamics, *Geophys. Res. Lett.*, *23*, 515–518.

Jickells, T. (1999), The inputs of dust derived elements to the Sargasso sea; a synthesis, *Mar. Chem.*, *68*, 5–14.

Kalnay, E., et al. (1996), The NCEP/NCAR 40-year reanalysis project, *Bull. Am. Meteorol. Soc.*, *77*, 437–471.

Kiss, P., I. Janosi, and O. Torres (2007), Early calibration problems detected in TOMS Earth-Probe aerosol signal, *Geophys. Res. Lett.*, *34*, L07803, doi:10.1029/2006GL028108.

Landsea, C., and W. Gray (1992), The strong association between western Sahelian monsoon rainfall and intense Atlantic hurricanes, *J. Clim.*, *5*, 435–453.

Lau, W. K. M., and K.-M. Kim (2007), How nature foiled the 2006 hurricane forecasts, *Eos Trans. AGU*, *88*(9), 105.

Levin, Z., A. Teller, E. Ganor, and Y. Yin (2005), On the interactions of mineral dust, sea-salt particles, and clouds: A measurement and modeling study from the Mediterranean Israeli Dust Experiment campaign, *J. Geophys. Res.*, *110*, D20202, doi:10.1029/2005JD005810.

Lydolph, P. (1985), *The Climate of the Earth*, 385 pp., Rowman and Littlefield, Totowa, N.J.

Mahowald, N. M., C. S. Zender, C. Luo, D. Savoie, O. Torres, and J. del Corral (2002), Understanding the 30-year Barbados desert dust record, *J. Geophys. Res.*, *107*(D21), 4561, doi:10.1029/2002JD002097.

Mahowald, N., C. Lou, J. del Corral, and C. S. Zender (2003), Interannual variability in atmospheric mineral aerosols from a 22-year model simulation and observational data, *J. Geophys. Res.*, *108*(D12), 4352, doi:10.1029/2002JD002821.

Massie, S. T., O. Torres, and S. J. Smith (2004), Total Ozone Mapping Spectrometer (TOMS) observations of increases in Asian aerosol in winter from 1979 to 2000, *J. Geophys. Res.*, *109*, D18211, doi:10.1029/2004JD004620.

Mo, K., and R. Livezey (1986), Tropical-extratropical geopotential height teleconnection during the Northern Hemisphere winter, *Mon. Weather Rev.*, *114*, 2488–2515.

Moulin, C., C. Lambert, F. Dulac, and U. Dayan (1997), Control of atmospheric export of dust from North Africa by the North Atlantic Oscillation, *Nature*, *387*, 691–694.

Palmer, T. (1986), Influence of the Atlantic, Pacific and Indian oceans on Sahel rainfall, *Nature*, *322*, 251–253.

Petit, R. H., M. Legrand, I. Jankowiak, J. Molinié, C. Asselin de Beauville, G. Marion, and J. L. Mansot (2005), Transport of Saharan dust over the Caribbean islands: Study on an event, *J. Geophys. Res.*, *110*, D18S09, doi:10.1029/2004JD004748.

Piontkovski, S., and S. Hameed (2002), Precursors of copepod abundance in the Gulf of Maine in atmospheric centers of action and sea surface temperature, *Global Atmos. Ocean Syst.*, *8*, 283–291.

Prospero, J. (1999), Long-range transport of mineral dust in the global atmosphere: Impact of African dust on the environment of the southeastern United States, *Proc. Natl. Acad. Sci. U. S. A.*, *96*, 3396–3403.

Prospero, J. M., and T. N. Carlson (1972), Vertical and areal distribution of Saharan dust over the western equatorial North Atlantic Ocean, *J. Geophys. Res.*, *77*, 5255–5265.

Prospero, J., and P. Lamb (2003), African droughts and dust transport to the Carribean: Climate change implications, *Science*, *302*, 1024–1027.

Prospero, J., and R. Nees (1986), Impact of the North African drought and El Niño on mineral dust in the Barbados trade winds, *Nature*, *320*, 735–738.

Prospero, J., P. Ginoux, O. Torres, S. Nicholson, and T. Gill (2002), Environmental characterization of global sources of atmospheric soil dust identified with the Nimbus 7 Total Ozone Mapping Spectromenter (TOMS) absorbing aerosol product, *Rev. Geophys.*, *40*(1), 1002, doi:10.1029/2000RG000095.

Riemer, N., O. M. Doherty, and S. Hameed (2006), On the variability of African dust transport across the Atlantic, *Geophys. Res. Lett.*, *33*, L13814, doi:10.1029/2006GL026163.

Rosenfeld, D., Y. Rudich, and R. Lahav (2001), Desert dust suppressing precipitation: A possible desertification feedback loop, *Proc. Natl. Acad. Sci. U. S. A.*, *98*, 5975–5980.

Rossby, C.-G. (1939), Relation between variations in the intensity of the zonal circulation of the atmosphere and the displacement of the semipermanent centers of actions, *J. Mar. Res.*, *2*, 38–55.

Rowell, D. (2001), Teleconnections between the tropical Pacific and the Sahel, *Q. J. R. Meteorol. Soc.*, *127*, 1683–1706.

Shi, W. (1999), On the relationship between the interannual variability of the Northern Hemispheric subtropical highs and the east-west divergent circulation during summer, Ph.D. thesis, Stony Brook Univ., Stony Brook, N.Y.

Torres, O., P. Bhartia, J. Herman, Z. Ahmad, and J. Gleason (1998), Derivation of aerosol properties from satellite measurements of backscattered ultraviolet radiation: Theoretical basis, *J. Geophys. Res.*, *103*, 17,099–17,110.

Torres, O., P. Bhartia, J. Herman, A. Sinyuk, P. Ginoux, and B. Holben (2002), A long-term record of aerosol optical depth from TOMS observation and comparison to AERONET measurements, *J. Atmos. Sci.*, *59*, 398–413.

Trenberth, K., G. Branstator, D. Karoly, A. Kumar, N.-C. Lau, and C. Ropelewski (1998), Progress during TOGA in understanding and modeling global teleconnections associated with tropical sea surface temperatures, *J. Geophys. Res.*, *103*, 14,291–14,324.

Wallace, J., and D. Gutzler (1981), Teleconnections in the geopotential height field during the Northern Hemisphere winter, *Mon. Weather Rev.*, *109*, 784–812.

Washington, R., and M. C. Todd (2005), Atmospheric controls on mineral dust emission from the Bodélé Depression, Chad: The role of the low level jet, *Geophys. Res. Lett.*, *32*, L17701, doi:10.1029/2005GL023597.

Zhao, P., Y. Zhu, and R. Zhang (2007), An Asian-Pacific teleconnection in summer tropospheric temperature and associated Asian climate variability, *Clim. Dyn.*, *29*, 293–303.

O. M. Doherty and S. Hameed, School of Marine and Atmospheric Science, Stony Brook University, Stony Brook, NY 11794-5000, USA. (nicole.riemer@stonybrook.edu)

N. Riemer, Department of Atmospheric Sciences, University of Illinois at Urbana-Champaign, 105 S. Gregory Street, M/C 223, Urbana, IL 61801, USA. (nriemer@uiuc.edu)